1198–1204 *Nucleic Acids Research, 1998, Vol. 26, No. 5*

Mutational analysis of the $tRNA_3^{Lys}$/HIV-1 RNA (primer/template) complex

Catherine Isel[+], Gérard Keith, Bernard Ehresmann, Chantal Ehresmann and Roland Marquet*

Unité Propre de Recherche No. 9002 du Centre National de la Recherche Scientifique, Institut de Biologie Moléculaire et Cellulaire, 15 rue René Descartes, 67084 Strasbourg cedex, France

Received December 5, 1997; Revised and Accepted January 14, 1998

ABSTRACT

Retroviruses use a specific tRNA, whose 3′ end is complementary to the 18 nucleotides of the primer binding site (PBS), to prime reverse transcription. Previous work has shown that initiation of HIV-1 reverse transcription is a specific process, in contrast with the subsequent elongation phase. HIV-1 reverse transcriptase (RT) specifically recognizes the complex formed by the viral RNA and $tRNA_3^{Lys}$. We previously proposed a secondary structure model of this complex based on chemical and enzymatic probing. In this model, $tRNA_3^{Lys}$ extensively interacts with the genomic RNA. Here, we have combined site-directed mutagenesis and structural probing to test crucial aspects of this model. We found that the complex interactions between $tRNA_3^{Lys}$ and HIV-1 RNA, and the intra-molecular rearrangements did not depend on the presence of upstream and downstream viral sequences. Indeed, a short RNA template, encompassing nucleotides 123–217 of the HIV-1 Mal genome, was able, together with the primer tRNA, to adopt the same structure as longer viral RNA fragments. This model primer/template is thus amenable to detailed structural and functional studies. The probing data obtained on the $tRNA_3^{Lys}$/mutant viral RNA complexes support the previously proposed model. Furthermore, they indicate that destroying the complementarity between the anticodon of $tRNA_3^{Lys}$ and the so-called viral 'A-rich loop' destabilizes all four helices of the extended $tRNA_3^{Lys}$/HIV-1 RNA interactions.

INTRODUCTION

Reverse transcription is a central event in the retroviral life cycle (1,2). During this process, the dimeric genomic RNA (3) is converted into double-stranded DNA through a complex series of steps (4) that require a multifunctional enzyme, reverse transcriptase (RT), which possesses RNA- and DNA-dependent DNA polymerase and RNase H activities and also directs strand transfers (5). In retroviruses, initiation of reverse transcription is primed by a cellular tRNA, which is selectively encapsidated during budding of the viral particles (6).

Different classes of retroviruses use different primer tRNAs: e.g. $tRNA_3^{Lys}$, $tRNA_{1,2}^{Lys}$ and $tRNA^{Trp}$ are the natural primers of immunodeficiency viruses, including the human immunodeficiency virus type 1 (HIV-1), spumaretroviruses, and leukemia and sarcoma viruses, respectively (6). In all cases, the 3′ terminal 18 nucleotides (nt) of the primer are strictly complementary to the so called 'primer binding site' (PBS) located in the 5′ untranslated region of the genomic RNA. The newly synthesized (–) strand DNA is covalently linked to the 3′ end of the primer tRNA (5,6). In addition to this general tRNA/PBS interaction, evidence has accumulated for virus-specific interactions between the primer tRNA and the genomic RNA of avian retroviruses (7–10), HIV-1 (11–13) and the yeast retrotransposon Ty1 (14–16). These additional virus-specific interactions seem to be required for efficient replication (9,16–18), suggesting that they are directly involved in the initiation of reverse transcription.

We previously used extensive enzymatic and chemical probing to study the solution structure of HIV-1 RNA/$tRNA_3^{Lys}$ complex (11,12). These studies allowed us to propose a secondary structure model of the primer/template complex (12) (Fig. 1). Formation of the HIV-1 RNA/$tRNA_3^{Lys}$ complex is accompanied by numerous intra- and inter-molecular rearrangements that result in a highly structured complex. In addition to the interaction of the 18 3′ terminal nucleotides of $tRNA_3^{Lys}$ with the PBS, this secondary structure model suggests that the anticodon loop, the 3′ part of the anticodon stem and part of the variable loop of $tRNA_3^{Lys}$ interact with viral sequences located upstream of the PBS (12) (Fig. 1). Interestingly, these interactions require the post-transcriptional modifications of $tRNA_3^{Lys}$, in particular $mcm^5s^2U_{34}$ (S_{34}) for stability of the complex (11).

These extended interactions probably explain the specificity of the initiation of reverse transcription observed both *in vitro* and in cell culture. *In vitro*, extension of natural $tRNA_3^{Lys}$ is much more efficient than that of a synthetic $tRNA_3^{Lys}$ lacking post-transcriptional modifications, and of an 18mer oligoribonucleotide complementary to the PBS (19–21). The HIV-1 RNA/$tRNA_3^{Lys}$ complex is efficiently extended by HIV-1 RT, but not by heterologous RTs, including those of other lentiviruses that

*To whom correspondence should be addressed. Tel: +33 3 88 41 70 91; Fax: +33 3 88 60 22 18; Email: marquet@ibmc.u-strasbg.fr

[+]Present address: MRC, Laboratory of Molecular Biology, Hills Road, Cambridge CB2 2QH, UK

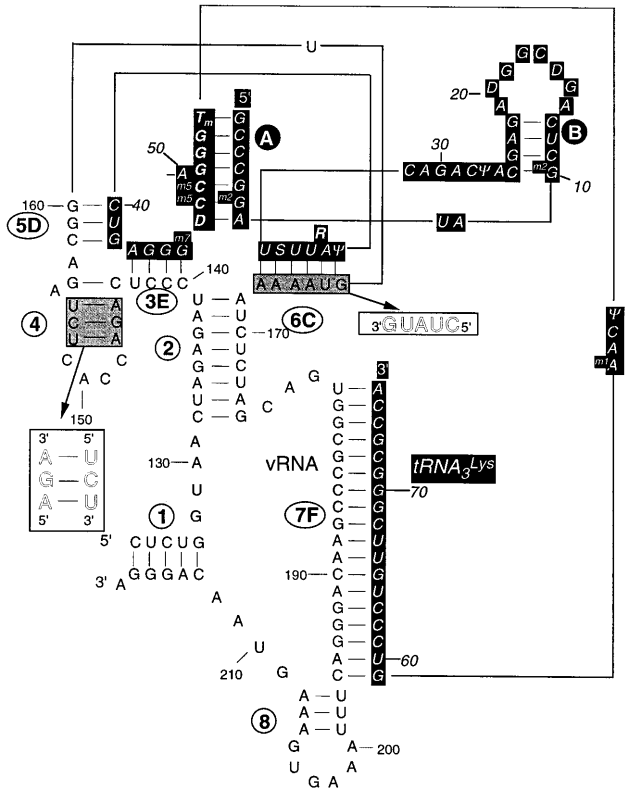

Figure 1. Secondary structure model of the HIV-1 vRNA/tRNA$_3^{Lys}$ complex. The tRNA sequence is in white on a black background. The region of the vRNA corresponding to nt 123–217 of the HIV-1 genome (MAL isolate) is represented. Helices are numbered according to Isel *et al.* (12). Mutations that were introduced in order to test the existence of helices 4 and 6C are shown.

have the same natural primer (19,22). Conversely, HIV-1 RT is unable to efficiently extend tRNA$_{1,2}^{Lys}$, tRNA^{Trp}, tRNA^{Pro}, tRNA^{Phe} and tRNA^{Ile} annealed to HIV-1 RNAs whose PBSs are mutated to be complementary to the 3′ end of those primers (23,24). Likewise, mutating the PBS does not suffice to stably change the primer usage of HIV-1 in cell culture (23,25,26). Indeed, complementarity between the anticodon loop of the tRNA and the so called A-rich loop located upstream of the PBS is required for efficient replication of HIV-1 (17,18,27). This particular point is predicted by our secondary structure model (Fig. 1). However, other nucleotides in the U5 region have also been proposed to be involved in the primer selection and maintenance *in vivo* (28,29).

In this report, we have combined site-directed mutagenesis and structural probing to test the secondary structure model of the HIV-1 RNA/tRNA$_3^{Lys}$ complex. First, we constructed a minimal template RNA still able to form the complex primer/template structure, and compared the complexes formed with tRNA$_3^{Lys}$ by this and a longer template RNA. In addition, we tested critical aspects of the secondary structure model by analyzing the conformation of binary complexes containing mutant templates. Our results fully support the model presented in Figure 1 and are discussed in light of the data obtained from HIV-1 replication in cell culture. Furthermore, our finding that the primer/template folds into an independent structural domain suggests that the short template used here constitutes, with the tRNA$_3^{Lys}$ primer, a good model system for further structural and functional studies.

MATERIALS AND METHODS

Templates and primer

Wild type RNA templates corresponding to nt 1–311 or 123–217 of HIV-1 (Mal isolate) were synthesized by *in vitro* transcription with the RNA polymerase from phage T7 of plasmids pJCB (30) or pICSN (13) cut with *Rsa*I or *Sma*I, respectively, as previously described (31). RNAs 1–311 mutated in helices 4 and 6C were obtained by *in vitro* transcription of plasmids pICHx4 and pICHx6C, respectively. In pICHx4, nucleotides $_{145}$AGA$_{147}$ and $_{152}$TCT$_{154}$ were replaced by $_{145}$TCT$_{147}$ and $_{152}$AGA$_{154}$. In pICHx6C, the sequence CTATG was substituted for $_{162}$GTAAAA$_{167}$. These plasmids were constructed from plasmid pJCB by inverse PCR. The PCR products were purified by gel electrophoresis, phosphorylated and used to transform JM109 *Escherichia coli* cells after ligation. Purification of wild type and mutant HIV-1 RNAs and of bovine tRNA$_3^{Lys}$ was as described elsewhere (11). Annealing of wild type and mutant HIV-1 RNAs to tRNA$_3^{Lys}$ was previously described (11,12).

Chemical and enzymatic probing of viral RNA

Modifications of 123–217 and of 1–311 viral RNAs (vRNAs) mutated in helices 4 and 6C with dimethyl sulfate (DMS), 1-cyclohexyl-*N*′-[2-(*N*-methylmorpholino)]ethyl-carbodiimide-*p*-toluenesulfonate (CMCT), RNase V1 and the *Neurospora crassa* endonuclease were performed as previously described for wild type 1–311 RNA (12). Modified bases and positions of cleavage were detected by primer extension assay as previously described (32)

Enzymatic probing of tRNA$_3^{Lys}$

Probing with *N.crassa* endonuclease and RNase V1 of tRNA$_3^{Lys}$ involved in the binary complex with either wild type or mutated 1–311 RNAs or with 123–217 RNA was as described elsewhere (11,12). After ethanol precipitation, the cleavage sites were identified by electrophoresis on a 15% denaturing polyacrylamide gel.

RESULTS

Experimental strategy

The secondary structure model of the HIV-1 RNA/tRNA$_3^{Lys}$ complex (Fig. 1) is based on extensive structural probing (12). One of the Watson–Crick positions of each nucleotide of the RNA corresponding to nt 1–311 of the HIV-1 genome was tested with chemical probes. The vRNA was also tested with RNase T2 and RNase V1. The conformation of tRNA$_3^{Lys}$ was tested with S1 and *N.crassa* endonucleases and with RNase V1. The accessibility of the N3 position of C residues and N7 position of A residues of tRNA$_3^{Lys}$ were tested with chemical probes (12).

The goals of the present study were 2-fold. First, we wanted to test whether the secondary structure depicted in Figure 1 was independent of the rest of the vRNA. For this purpose, we constructed a vRNA fragment corresponding to nt 123–217 of the genomic RNA of HIV-1 (Mal) and we compared the secondary structures of the 123–217 vRNA/tRNA$_3^{Lys}$ complex to that obtained when using a large fragment of the genomic RNA (1–311 RNA). The conformation of the primer/template complex obtained with 123–217 vRNA also provides a direct test of the secondary structure model. Second, we tested aspects of the

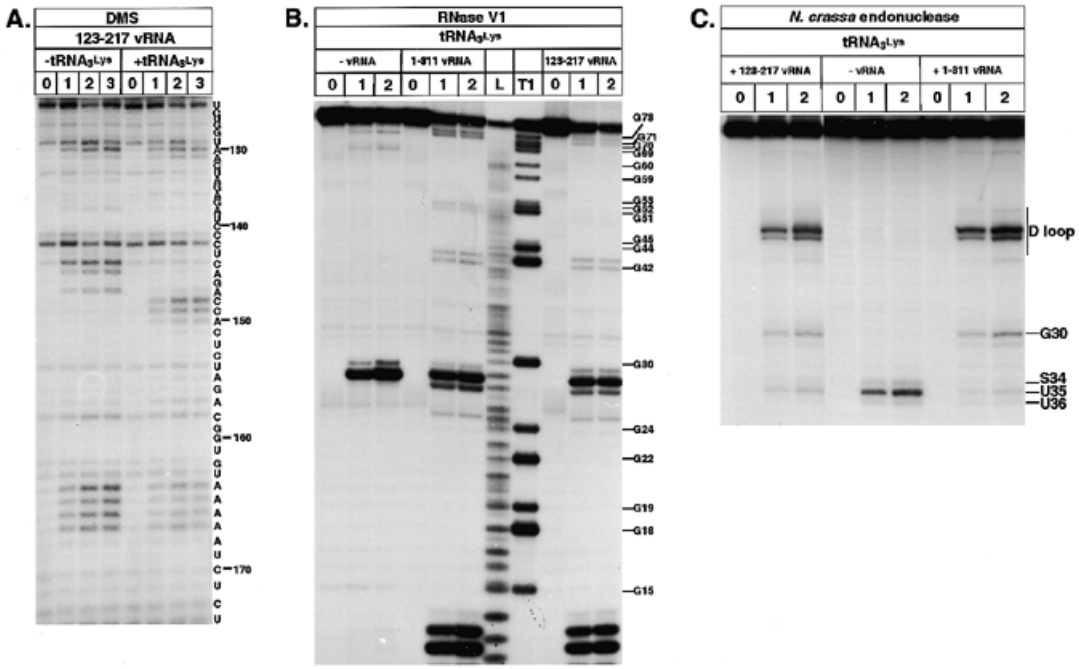

Figure 2. Chemical and enzymatic probing of the primer/template complex formed by $tRNA_3^{Lys}$ and 123–217 vRNA. (**A**) 123–217 vRNA, either in the free form (left) or in the primer/template complex (right) was tested with DMS. Lanes indicated by 0 are controls incubated in the absence of the chemical probes. Lanes 1, 2 and 3 correspond to modifications for 5, 10 and 15 min, respectively. (**B**) 5′ end-labelled $tRNA_3^{Lys}$, either free (left) or bound to wild type 1–311 (middle) or 123–217 (right) vRNAs, was probed with RNase V1. Lanes indicated by 0 are controls incubated in the absence of RNase. Lanes 1 and 2 correspond to incubation with 0.045 U of RNase V1 for 5 and 10 min, respectively. Lanes denoted L and T1 are ladders obtained by alkaline hydrolysis and RNase T1 hydrolysis at acidic pH, respectively. (**C**) 3′ end-labelled $tRNA_3^{Lys}$, either free (left) or bound to wild type 1–311 (middle) or 123–217 (right) vRNAs, was subjected to hydrolysis with 0.6 U of the *N.crassa* endonuclease for 5 or 10 min, respectively. Lane numbering is as in (B).

secondary structure model that are crucial for the global folding of the complex by site-directed mutagenesis. Indeed, critical testing of the secondary structure model is required to allow confident modelling of the three-dimensional structure of the primer/template complex. In the present study, the conformation of the wild type and mutant viral RNAs was tested with DMS, which reacts with position N1 of unpaired As and position N3 of unpaired Cs, and CMCT, which modifies position N1 of unpaired Gs and position N3 of unpaired Us. Thus, these two probes tested the chemical accessibility of one of the Watson–Crick positions of each nucleotide of the vRNA (33). The conformation of $tRNA_3^{Lys}$, either free or annealed to wild type and mutant vRNA, was tested with RNase V1, which preferentially cleaves double-stranded regions, and the single strand-specific S1 and *N.crassa* endonucleases (33). Since the probing data obtained on the wild type primer/template have been discussed in detail elsewhere (12), we focus here on the data obtained with the mutant templates. However, our conclusions are based on the direct comparison between the two data sets.

A minimal vRNA fragment accounts for the complex primer/template interactions

According to the previously published secondary structure model, the same binary complex should be obtained using templates corresponding either to nt 1–311 or 123–217 of HIV-1. We tested the binary complex formed between 123–217 vRNA and $tRNA_3^{Lys}$ with chemical and enzymatic probes (Fig. 2 and data not shown). With wild type 1–311 vRNA, the most informative data reflecting formation of the primer/template were obtained with DMS in the region upstream from the PBS (11,12). The corresponding experiment using 123–217 vRNA is shown in Figure 2A. Upon formation of the 123–217 vRNA/$tRNA_3^{Lys}$ complex, reactivity decreases are observed at $_{167}$AAAA$_{164}$, A_{147}, $_{145}$AC$_{144}$ and A_{138}. As previously observed with 1–311 vRNA, the protection of $_{167}$AAAA$_{164}$ is not complete, reflecting the dynamic nature of helix 6C (11,12). Protections at positions 138, 144–145 and 147 of the vRNA are compatible with formation of helices 2 and 4 (Fig. 1). Likewise, the unpaired $_{130}$AA$_{131}$ remain accessible to DMS and the reactivity increase at $_{148}$CCA$_{150}$ further supports the existence of stem–loop 4 (Figs 1 and 2). The reactivity increase at A_{157} is also compatible with the secondary structure model. Compared with the data previously obtained with 1–311 vRNA (11,12), the reactivity changes described here using 123–217 vRNA show that the same vRNA/$tRNA_3^{Lys}$ complex is formed independently of the template length.

The primer $tRNA_3^{Lys}$ was probed with RNase V1 (Fig. 2B), either in the free form or hybridized to 1–311 or 123–217 vRNA. In the free form, the main RNase V1 cleavages are observed at $_{28}$CpApG$_{30}$, in the anticodon stem, and in the 3′ part of the acceptor stem (Fig. 2B). The RNase V1 cleavage patterns of $tRNA_3^{Lys}$ bound to 1–311 and 123–217 vRNAs are very similar to each other and distinct from the cleavage pattern of free tRNA (Fig. 2B). Strong cleavages are observed at the 3′ end of helix 7F (at $_{71}$GpCpG$_{73}$), in helix B (at $_{12}$UpCpA$_{14}$), in the single-stranded junction between helices B and 6C (at $_{27}$ΨpCpApG$_{30}$), in helix 5D (at $_{41}$UpGpA$_{43}$) and on the 5′ strand of helix A (at $_{5}$Gp^{m2}GpA$_{7}$, not shown). The cleavages at $_{27}$ΨpCpApG$_{30}$ are

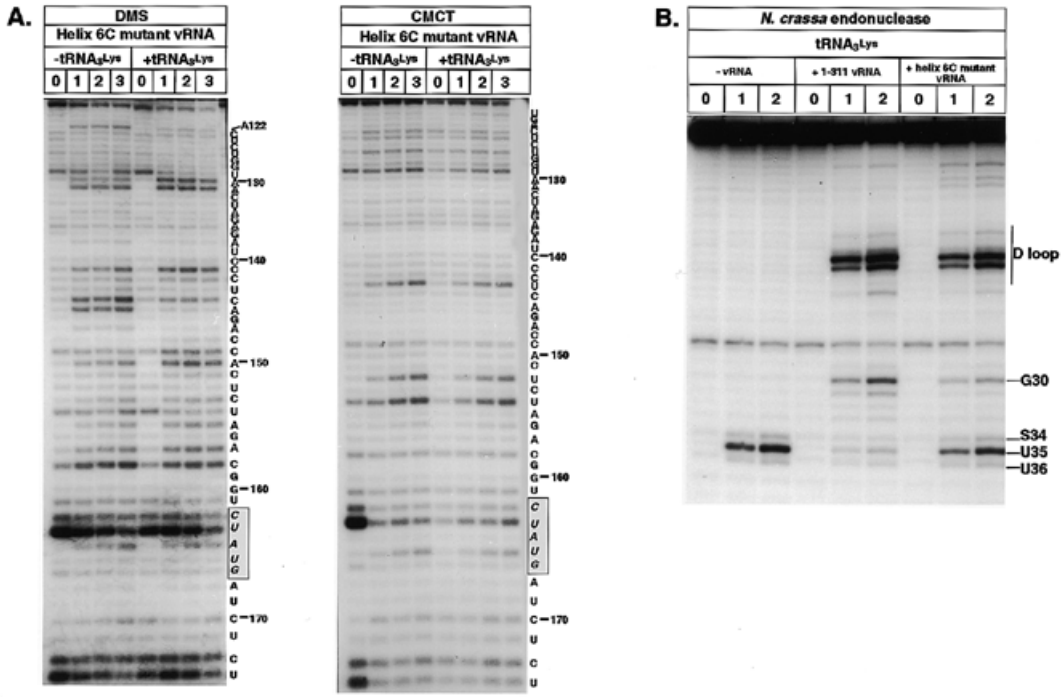

Figure 3. Chemical and enzymatic probing of the primer/template complex formed by $tRNA_3^{Lys}$ and helix 6C mutant vRNA. (**A**) Helix 6C mutant vRNA was used to form the primer/template complex and tested with DMS (left) and CMCT (right). Lanes indicated by 0 are controls incubated in the absence of the chemical probes. Lanes 1, 2 and 3 correspond to modifications for 10, 15 and 20 min (DMS treatment) or for 15, 30 and 45 min (CMCT treatment). The modified nucleotides were identified by extension of a DNA primer complementary to the PBS. (**B**) 3′ end-labelled $tRNA_3^{Lys}$, either free (left), bound to wild type 1–311 (middle) or bound to helix 6C mutant (right) vRNAs, was subjected to hydrolysis by *N.crassa* endonuclease. Experimental conditions and lane numbering are as in Figure 2C.

probably due to stacking of this single-stranded region (12). Cleavages by RNase V1 are also observed in the 3′ strand of helix A (at $_{50}$ApGpG$_{52}$). For unknown reasons, these cleavages are substantially stronger when $tRNA_3^{Lys}$ is annealed to 1–311 vRNA, than when using 123–217 vRNA as template. The same cleavage pattern was obtained with 3′ end-labelled tRNA instead of 5′ end-labelled $tRNA_3^{Lys}$ (data not shown).

In parallel, the conformation of $tRNA_3^{Lys}$ was tested with the *N.crassa* endonuclease (Fig. 2C). In the free tRNA, one strong and two weak cleavages are observed in the anticodon loop, at $_{34}$SUU$_{36}$. When $tRNA_3^{Lys}$ is annealed to either 1–311 or 123–317 vRNA, the same cleavage patterns are observed (Fig. 2C). The $tRNA_3^{Lys}$ anticodon is strongly protected from cleavage due to formation of helix 6C. At the same time, strong cleavages by *N.crassa* endonuclease are observed at $_{29}$ApG$_{30}$ and in the dihydrouridine loop, at $_{17}$CpGpG$_{19}$. The latter cleavages result from the opening of the tertiary interactions between the dihydrouridine and TΨ loops of $tRNA_3^{Lys}$, due to formation of helix 7F.

Taken together, our probing data indicate that the primer/template complex formed by $tRNA_3^{Lys}$ and either 1–311 or 123–217 vRNA adopt the same secondary structure.

Helix 6C stabilizes helices 3E, 4 and 5D

Helix 6C corresponds to the interaction of the anticodon loop of $tRNA_3^{Lys}$ and a conserved A-rich sequence located upstream from the PBS (Fig. 1), which is located in a loop in the free HIV-1 RNA, and is hence termed the A-rich loop (32). Nucleotides $_{162}$GUAAAA$_{167}$ of 1–311 vRNA were mutated to CUAUG, and the binary complex obtained with helix 6C mutant vRNA was probed with chemicals and RNases.

Probing of the mutant vRNA is consistent with the disruption of helix 6C in the primer/mutant vRNA complex (Fig. 3 and data not shown). Indeed, mutated nucleotides U$_{163}$, U$_{165}$ and A$_{164}$ are either strongly or moderately modified by CMCT and DMS, respectively, indicating that the mutated sequence adopts a single-stranded conformation in the primer/template complex (Fig. 3A). In addition, strong reactivities at C$_{141}$, U$_{143}$, C$_{144}$ and $_{150}$ACUCUAGAC$_{158}$ in the mutant vRNA reveals disruption of helices 3E, 4 and 5D (Fig. 3A). Besides, our probing data support the existence of helices 1, 2, 7F and 8 (Fig. 3 and data not shown). For example, the reactivity of nucleotides $_{132}$CUAGAGAU$_{139}$ and $_{168}$AUCUCUAG$_{175}$ is very low, as predicted if helix 2 is formed (Fig. 3A and B). (In some cases, the reactivity cannot be determined because of stops in the primer extension assay that are present even in the absence of chemical probe). Since most of these nucleotides are also unreactive in the free vRNA (Fig. 3A and B) (12), the absence of reactivity in the binary complex might also reflect the persistence of some initial structure, such as the upper part of the A-rich loop hairpin (12). However, the reactivity increase of A$_{155}$ and A$_{157}$ upon formation of the primer/template complex reflects a rearrangement of the viral A-rich stem–loop that is compatible with formation of helix 2 (12). Similarly, nucleotides $_{123}$CUCUG$_{127}$, which are involved in helix 1 are almost completely protected from chemical modification (Fig. 3A and B).

The conformation of $tRNA_3^{Lys}$ was tested with the *N.crassa* endonuclease (Fig. 3B). Contrary to what was observed when the primer tRNA is annealed with wild type vRNA, the anticodon of

tRNA$_3^{Lys}$ annealed to helix 6C mutant vRNA is cleaved by *N.crassa* endonuclease to an extent similar to that of free tRNA$_3^{Lys}$. This result confirms that, as expected from the secondary structure model, the anticodon loop of tRNA$_3^{Lys}$ is single-stranded in the mutant binary complex. This is in keeping with probing experiments of tRNA$_3^{Lys}$ with nuclease S1 that showed that the mutation in the vRNA destroys helix 6C (19). These data indicated that helix 5D is also destroyed by the mutation, while helices A, B and 7F are conserved (19). The cleavage intensities at G_{18} and G_{19} in the D-loop (loop B) are similar when tRNA$_3^{Lys}$ is bound to either wild type or helix 6C mutant vRNAs. However, the cleavage at G_{30} is decreased in the tRNA/mutant vRNA complex. Indeed, in the absence of helices 6C and 5D, the anticodon stem of tRNA$_3^{Lys}$ might not be completely open.

Taken together, our probing data on the binary complex formed with the helix 6C mutant vRNA support the proposed secondary structure model. In addition, the results obtained with this mutated vRNA indicate that helices 3E, 4 and 5D are unstable in the absence of helix 6C.

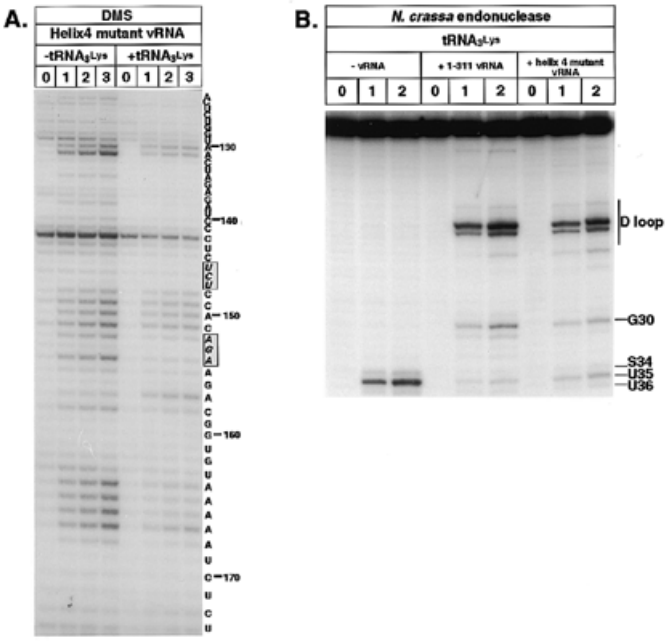

Figure 4. Chemical and enzymatic probing of the primer/template complex formed by tRNA$_3^{Lys}$ and helix 4 mutant vRNA. (**A**) Helix 4 mutant vRNA, either free (left) or bound to tRNA$_3^{Lys}$ (right), was probed with DMS. Experimental conditions and lane numbering are as in Figure 2A. (**B**) 3′ end-labelled tRNA$_3^{Lys}$, either free (left), or bound to wild type (middle) and mutant vRNA (right), was probed with the endonuclease from *N.crassa*. Experimental conditions and lane numbering are as in Figure 2C.

Existence of stem–loop 4

A mutant vRNA was constructed to test the existence of stem–loop 4. Indeed, it is possible to propose an alternative secondary structure model of the primer/template complex in which helix 3E would be extended by base-pairing nucleotides $_{144}$CAGA$_{147}$ of the vRNA with the $_{39}$ΨCUG$_{42}$ sequence in tRNA$_3^{Lys}$, while $_{152}$UCUAGA$_{157}$ would be associated with $_{27}$ΨCAGA$_{31}$, with A_{155} bulging out (Fig. 1). These interactions are incompatible with the existence of helices 4 and 5D and would strongly affect the three-dimensional structure of the junction between helices 2, 3E, A and 6C that constitutes the core of the secondary structure model.

In order to test the existence of helix 4, sequences $_{145}$AGA$_{147}$ and $_{152}$UCU$_{154}$ were exchanged, thus maintaining complementarity in the putative helix 4 while preventing the alternative base-pairings (Fig. 1). This mutant vRNA and tRNA$_3^{Lys}$ involved in the binary complex were tested with chemicals and nucleases (V1, S1 and *N.crassa* endonuclease), respectively (Fig. 4 and data not shown). Probing of the mutated region with DMS and CMCT indicates that nt 145–154 adopt a stem–loop structure in the tRNA$_3^{Lys}$/helix 4 mutant vRNA complex (Fig. 4A and data not shown). Mutated nucleotides C146, A152 and A154 are protected from modification with DMS, while the $_{148}$CCAC$_{151}$ sequence located in the loop of stem 4 is fully modified (Fig. 4A). The strong reactivity decreases at C_{158} and $_{164}$AAAA$_{167}$, and the reactivity increase at A_{157} upon formation of the binary complex (Fig. 4A) were identical to those observed when using the wild type vRNA (12), thus reflecting formation of helices 4, 5D and 6C.

Probing tRNA$_3^{Lys}$ with V1, S1 and *N.crassa* endonucleases (Fig. 4B and data not shown) revealed no differences between the binary complexes formed with either the wild type or the mutated vRNA, thus confirming the secondary structure model of Figure 1. For example, the cleavages induced by *N.crassa* endonuclease at G_{18}, G_{19}, G_{30} and U_{35} have the same intensities using either wild type or helix 4 mutant vRNA being used as template (Fig. 4B).

DISCUSSION

We previously proposed a secondary structure model of the tRNA$_3^{Lys}$/HIV-1 vRNA complex based on extensive structural probing. The present data show that, as expected from this model, a vRNA fragment corresponding to nt 123–217 of HIV-1 genome can fold into this structure independently of the rest of the genomic RNA. These data do not rule out the possibility that sequences flanking the 123–217 region might be involved in binding of HIV-1 reverse transcriptase. However, we were unable to detect contacts between reverse transcriptase and viral RNA outside this region using enzymatic footprinting (C. Isel *et al.*, in preparation). In addition, these data revealed no or little effect of reverse transcriptase on the structure of the primer/template complex. Our structural data obtained on binary complexes containing mutant vRNAs further support the model by attesting to the existence of helices 6C and 4. Demonstrating the existence of helix 4 was important in order to eliminate alternative conformations that would impose quite different junctions between the other secondary structure elements.

The results obtained with helix 6C mutant vRNA are consistent with our previous observation that dethiolation of mcm^{5}s^{2}U34 (S34) in tRNA$_3^{Lys}$ strongly enhances reactivity of A_{166} towards DMS in wild type vRNA (11). An important result is that substitution of nt 162–167 not only results in disruption of helix 6C, but also of helices 3E, 4 and 5D. This observation indicates that helices 3E, 4, 5D and 6C probably belong to the same three-dimensional structural domain.

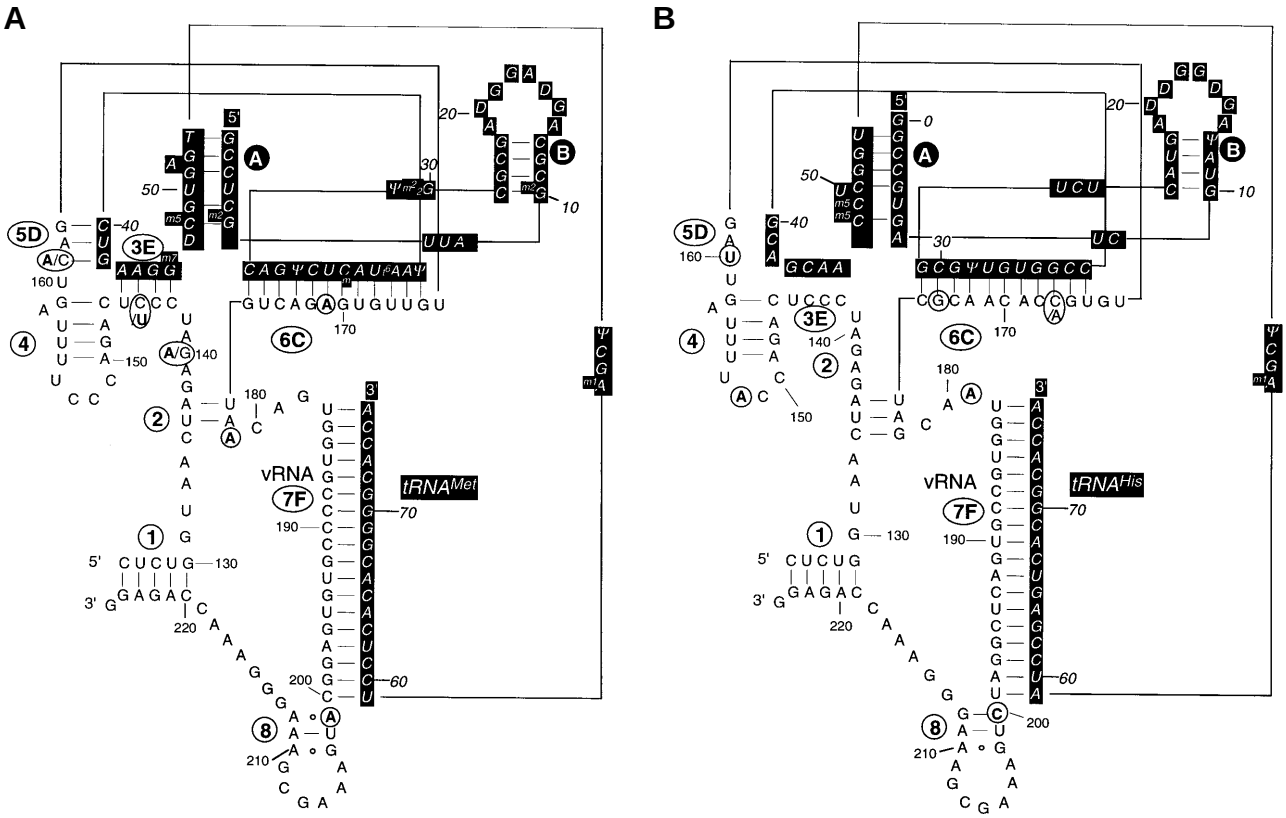

Figure 5. Hypothetical secondary structures of the tRNA/mutant vRNA complexes formed by mutant vRNAs stably maintaining a PBS complementary to $tRNA^{Met}$ (18) (**A**) or $tRNA^{His}$ (17,28,29) (**B**). The secondary structure model of Figure 1 was first modified to accommodate the sequence of wild type HIV HXB2 RNA. Then, the models were modified to account for the mutations introduced by Morrow and co-workers and for the primer change. The bold circled nucleotides correspond to nucleotide substitutions that were not initially introduced by site-directed mutagenesis but were selected upon prolonged cell culture. Numbering of the vRNA is according to Morrow and co-workers. Numbering of the tRNAs follows international rules (38) (e.g. the additional nucleotide at the 5′ end of $tRNA^{His}$ is G_0).

A classical way to demonstrate the existence of helix 6C would have been to use the helix 6C mutant vRNA and to introduce complementary mutations in the anticodon loop of $tRNA_3^{Lys}$. This strategy is not easily applicable here, since the complex intermolecular interactions (including helix 6C) are not stable when using an *in vitro* synthesized $tRNA_3^{Lys}$ lacking the post-transcriptional modifications of the natural primer (11,12). However, the existence of helix 6C has gained support from studies suggesting that the interaction between the viral A-rich loop and the anticodon loop of $tRNA_3^{Lys}$ is required for efficient replication of HIV-1. Indeed, it was shown that a $tRNA_3^{Lys}$ mutated in the anticodon loop is encapsidated in the HIV-1 particles (34), but is not efficiently used as primer in an endogenous reverse transcription assay (35). Similarly, deletion of the A-rich loop results in diminished levels of infectivity and reduced synthesis of viral DNA in MT-2 cells and cord blood mononuclear cells (27). Interestingly, the A-rich loop was reconstituted upon long term culture of the mutant virus (27). The structural evidence for the existence of helix 6C that we present here is also in agreement with our previous functional study, where we showed that the substitution of the A-rich sequence present in helix 6C vRNA produced a defect in the transition between the initiation and elongation phases of HIV-1 reverse transcription (19).

Further support for the importance of the extended interactions between $tRNA_3^{Lys}$ and HIV-1 RNA arose from experiments in which the HIV-1 PBS was altered to make it complementary to other tRNAs. Replication of the mutated viruses is dramatically reduced and reversion to the wild type PBS is rapidly observed (23,25,26). However, HIV-1 can stably maintain a PBS complementary to $tRNA^{His}$ (17,28,29) or $tRNA^{Met}$ (18), provided that the A-rich loop is also mutated to match to the anticodon loop of these tRNAs. Upon prolonged periods in cell culture, additional mutations, which suppress an initial replication defect, appeared in the vRNAs using these alternative tRNA primers (17,18,28,29) (Fig. 5).

We constructed hypothetical models of the secondary structures of the tRNA/mutant vRNA complexes formed by mutant vRNAs stably maintaining a PBS complementary to $tRNA^{Met}$ (18) (Fig. 5A) or $tRNA^{His}$ (17,28,29) (Fig. 5B). In both cases, helix 6C was maintained upon prolonged culture and no mutations were observed in helices 1 and 4. In the two mutants, helix 6C was extended, as compared with the interaction between wild type vRNA and $tRNA_3^{Lys}$, due to interactions between the 3′ strand of the anticodon stem of $tRNA^{Met}$ and $tRNA^{His}$ with the vRNA. In mutant vRNA maintaining a PBS^{Met}, a G to A mutation at position 170, which stabilizes helix 6C, was selected during long term culture (Fig. 5A) (18). In mutant vRNA stably maintaining a PBS^{His}, helix 6C was stabilized by selection of a U to G mutation at position 174 (18,28,29). In parallel, a C to A mutation at position 167, which introduces an A–G base-pair in helix 6C, was observed in some clones (Fig. 5B) (17). This non-canonical

base-pairing is well tolerated in RNA double helices (36). In mutant vRNA maintaining a PBS^{Met}, helices 3E and 5D were conserved (Fig. 5A). On the contrary, helices 3E and 5D could not be formed in the mutant vRNA maintaining a PBS^{His} (Fig. 5B). It is likely that the corresponding nucleotides are not simply in a single-stranded conformation but rather adopt alternative structures. For example, the anticodon stem of $tRNA^{His}$ could be maintained in the primer/template complex.

Taken together these results suggest that helices 6C and 7F are the only intermolecular interactions that are absolutely required for replication of HIV-1, while helices 3E and 5D are dispensable. However, they do not exclude that the latter helices could be required for optimal initiation of reverse transcription. Indeed, since synthesis of the (–) strong stop DNA is much faster than the overall replication of HIV-1, it has not been proven that even a 10-fold decrease in the rate of initiation of reverse transcription would significantly affect the kinetics of replication. Thus, defining the exact functional role of helices 3E and 5D (if any) will require detailed study of the initiation of reverse transcription of mutant vRNA either in cell culture or *in vitro*.

The existence of helix 6C has been recently questioned because a similar interaction does not exist in simian immunodeficiency virus (SIV) (37). Our present data, together with the work of C. Morrow and co-workers (17,18,22,28,29), suggest that the structures of the HIV-1 RNA/$tRNA_3^{Lys}$ and SIV RNA/$tRNA_3^{Lys}$ complexes are significantly different. Indeed, it has been shown that SIV RT is unable to efficiently extend the HIV-1 RNA/$tRNA_3^{Lys}$ complex (22).

The results of the present study allow the design of minimal templates for functional and structural studies, including X-ray crystallography. Furthermore, confirmation of the secondary structure of the primer/template complex now allows its functional dissection and modelling of its tertiary structure.

ACKNOWLEDGEMENTS

We thank Delphine Mignot for technical assistance, Marat Yussupov for help with the tRNA purification, Jean-Marc Lanchy for discussions and Steve Lodmell for critical reading of the manuscript. This work was supported by the ANRS (Agence Nationale de Recherches sur le SIDA).

REFERENCES

1 Baltimore, D. (1970) *Nature*, **226**, 1209–1211.
2 Temin, H.M. and Mizutani, S. (1970) *Nature*, **226**, 1211–1213.
3 Paillart, J.C., Marquet, R., Skripkin, E., Ehresmann, C. and Ehresmann, B. (1996) *Biochimie*, **78**, 639–653.
4 Gilboa, E., Mitra, S.W., Goff, S. and Baltimore, D. (1979) *Cell*, **18**, 93–100.
5 Skalka, A.M. and Goff, S.P. (1993) *Reverse Transcriptase*. Cold Spring Harbor Laboratory Press, N.Y.
6 Marquet, R., Isel, C., Ehresmann, C. and Ehresmann, B. (1995) *Biochimie*, **77**, 113–124.
7 Cobrinik, D., Soskey, L. and Leis, J. (1988) *J. Virol.*, **62**, 3622–3630.
8 Cobrinik, D., Aiyar, A., Ge, Z., Katzman, M., Huang, H. and Leis, J. (1991) *J. Virol.*, **65**, 3864–3872.
9 Aiyar, A., Cobrinik, D., Ge, Z., Kung, H.J. and Leis, J. (1992) *J. Virol.*, **66**, 2464–2472.
10 Aiyar, A., Ge, Z. and Leis, J. (1994) *J. Virol.*, **68**, 611–618.
11 Isel, C., Marquet, R., Keith, G., Ehresmann, C. and Ehresmann, B. (1993) *J. Biol. Chem.*, **268**, 25269–25272.
12 Isel, C., Ehresmann, C., Keith, G., Ehresmann, B. and Marquet, R. (1995) *J. Mol. Biol.*, **247**, 236–250.
13 Skripkin, E., Isel, C., Marquet, R., Ehresmann, B. and Ehresmann, C. (1996) *Nucleic Acids Res.*, **24**, 509–514.
14 Friant, S., Heyman, T., Poch, O., Wilhelm, M. and Wilhelm, F.X. (1997) *Yeast*, **13**, 639–645.
15 Friant, S., Heyman, T., Wilhelm, M.L. and Wilhelm, F.X. (1996) *Nucleic Acids Res.*, **24**, 441–449.
16 Wilhelm, M., Wilhelm, F.X., Keith, G., Agoutin, B. and Heyman, T. (1994) *Nucleic Acids Res.*, **22**, 4560–4565.
17 Wakefield, J.K., Kang, S.-M. and Morrow, C.D. (1996) *J. Virol.*, **70**, 966–975.
18 Kang, S.M., Zhang, Z.J. and Morrow, C.D. (1997) *J. Virol.*, **71**, 207–217.
19 Isel, C., Lanchy, J.M., Le Grice, S.F.J., Ehresmann, C., Ehresmann, B. and Marquet, R. (1996) *EMBO J.*, **15**, 917–924.
20 Lanchy, J.M., Ehresmann, C., Le Grice, S.F.J., Ehresmann, B. and Marquet, R. (1996) *EMBO J.*, **15**, 7178–7187.
21 Arts, E.J., Ghosh, M., Jacques, P.S., Ehresmann, B. and Le Grice, S.F.J. (1996) *J. Biol. Chem.*, **271**, 9054–9061.
22 Arts, E.J., Stetor, S.R., Li, X.G., Rausch, J.W., Howard, K.J., Ehresmann, B., North, T.W., Wohrl, B.M., Goody, R.S., Wainberg, M.A. and Le Grice, S.F.J. (1996) *Proc. Natl. Acad. Sci. USA*, **93**, 10063–10068.
23 Li, X.G., Mak, J., Arts, E.J., Gu, Z.X., Kleiman, L., Wainberg, M.A. and Parniak, M.A. (1994) *J. Virol.*, **68**, 6198–6206.
24 Oude Essink, B.B., Das, A.T. and Berkhout, B. (1996) *J. Mol. Biol.*, **264**, 243–254.
25 Das, A.T., Klaver, B. and Berkhout, B. (1995) *J. Virol.*, **69**, 3090–3097.
26 Wakefield, J.K., Wolf, A.G. and Morrow, C.D. (1995) *J. Virol.*, **69**, 6021–6029.
27 Liang, C., Li, X., Rong, L., Inouye, P., Quan, Y., Kleiman, L. and Wainberg, M.A. (1997) *J. Virol.*, **71**, 5750–5757.
28 Zhang, Z.J., Kang, S.M., LeBlanc, A., Hajduk, S.L. and Morrow, C.D. (1996) *Virology*, **226**, 306–317.
29 Li, Y., Zhang, Z., Wakefield, J.K., Kang, S.M. and Morrow, C.D. (1997) *J. Virol.*, **71**, 6315–6322.
30 Paillart, J.C., Marquet, R., Skripkin, E., Ehresmann, B. and Ehresmann, C. (1994) *J. Biol. Chem.*, **269**, 27486–27493.
31 Marquet, R., Baudin, F., Gabus, C., Darlix, J.L., Mougel, M., Ehresmann, C. and Ehresmann, B. (1991) *Nucleic Acids Res.*, **19**, 2349–2357.
32 Baudin, F., Marquet, R., Isel, C., Darlix, J.L., Ehresmann, B. and Ehresmann, C. (1993) *J. Mol. Biol.*, **229**, 382–397.
33 Ehresmann, C., Baudin, F., Mougel, M., Romby, P., Ebel, J.P. and Ehresmann, B. (1987) *Nucleic Acids Res.*, **15**, 9109–9128.
34 Huang, Y., Mak, J., Cao, Q., Li, Z., Wainberg, M.A. and Kleiman, L. (1994) *J. Virol.*, **68**, 7676–7683.
35 Huang, Y., Shalom, A., Li, Z., Wang, J., Mak, J., Wainberg, M.A. and Kleiman, L. (1996) *J. Virol.*, **70**, 4700–4706.
36 Leonard, G.A., Mcauleyhecht, K.E., Ebel, S., Lough, D.M., Brown, T. and Hunter, W.N. (1994) *Structure*, **2**, 483–494.
37 Berkhout, B. (1997) *Nucleic Acids Res.*, **25**, 4013–4017.
38 Steinberg, S., Misch, A. and Sprintzl, M. (1993) *Nucleic Acids Res.*, **21**, 3011–3015.